IOPscience iopscience.iop.org

Home Search Collections Journals About Contact us My IOPscience

Evidence for interpenetrating magnetic structures across an IC-C phase transition in $Mn_{0.88}Fe_{0.12}WO_4$

This article has been downloaded from IOPscience. Please scroll down to see the full text article.

2001 J. Phys.: Condens. Matter 13 2753

(http://iopscience.iop.org/0953-8984/13/12/301)

View the table of contents for this issue, or go to the journal homepage for more

Download details:
IP Address: 171.66.16.226
The article was downloaded on 16/05/2010 at 11:43

Please note that terms and conditions apply.

INSTITUTE OF PHYSICS PUBLISHING JOURNAL OF PHYSICS: CONDENSED MATTER

J. Phys.: Condens. Matter **13** (2001) 2753–2766 www.iop.org/Journals/cm PII: S0953-8984(01)21027-3

Evidence for interpenetrating magnetic structures across an IC–C phase transition in $Mn_{0.88}Fe_{0.12}WO_4$

N Stüßer[1], Y Ding[1], M Hofmann[1], M Reehuis[1], B Ouladdiaf[1,2], G Ehlers[1], D Günther[1], M Meißner[1] and M Steiner[1]

[1] Hahn–Meitner Institut, D-14109 Berlin, Glienickerstrasse 100, Germany
[2] Institut Laue–Langevin, BP 156, F-38042 Grenoble, France

E-mail: stuesser@hmi.de

Received 17 January 2001

Abstract

Neutron diffraction, specific heat and magnetization measurements were applied to study the magnetic structures in $Mn_{0.88}Fe_{0.12}WO_4$ using single crystal and powder samples. A commensurate antiferromagnetic structure with a propagation vector $\boldsymbol{k} = (1/4, 1/2, 1/2)$ below 13.5 K and an incommensurate structure with $\boldsymbol{k} = (0.23, 0.5, 0.508)$ between 13.5 K and 15.5 K were found to be the dominating ordered states. The temperature behaviour of the propagation vector above the IC–C phase transition shows a logarithmic behaviour. An $FeWO_4$-type ordering of spins with $\boldsymbol{k} \approx (1/2, 0, 0)$ is observed below 19 K and coexists between 15.5 K and 13.5 K with the $MnWO_4$-type structure. Our experimental results indicate a cluster-like $FeWO_4$-type magnetic ordering on a diluted 3D lattice, which interpenetrates the dominating $MnWO_4$-type spin ordering. Below 13 K, with the majority of spins ordered in the commensurate $MnWO_4$-type structure, reflections which can be indexed to a unit cell doubled along the crystallographic a-axis appear again; however, these intensities cannot purely be related to Bragg diffraction by ordered local magnetic moments at the (Mn, Fe) positions.

1. Introduction

Studies on the crystal structure and the magnetic ordering in the series of mixed crystals $Mn_{1-x}Fe_xWO_4$ were performed in the 1960s and 1970s [1]. Pure $FeWO_4$ (ferberite) and $MnWO_4$ (huebnerite) are isostructural, crystallize in the monoclinic space group $P2/c$ and possess only small differences in lattice constants of about 1%. Both the 3d metals and the tungsten atoms are surrounded by distorted oxygen octahedra and form alternating layers in the bc-plane (figure 1). Despite their very similar chemical structure the magnetic structures of $FeWO_4$ and $MnWO_4$ are quite different.

The collinear antiferromagnetic (AF) magnetic ground state of $FeWO_4$ below $T_N = 76$ K is described by a propagation vector $\boldsymbol{k} = (1/2, 0, 0)$ and the moments are inclined by about 26°

 © 2001 IOP Publishing Ltd Printed in the UK

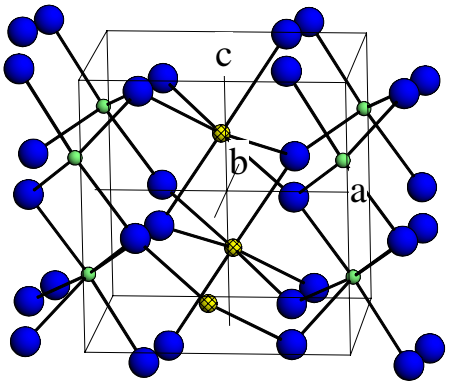

Figure 1. Structure of (Mn,Fe)WO_4. The $(Mn/Fe)^{2+}$ ions (small hatched circles) and the W^{6+} ions (small circles) are surrounded by distorted oxygen (large circles) octahedra. The frame indicates the unit cell.

to the a-axis in the ac-plane (figure 2(a)). It was only recently that the different magnetic phases of $MnWO_4$ were determined by neutron diffraction [1]. These measurements confirmed that the collinear AF magnetic ground state AF1 of $MnWO_4$ occurring below 8 K can be described by a propagation vector $\boldsymbol{k} = (0.25, 0.5, 0.5)$ (figure 2(b)). Similar to $FeWO_4$ the moments are again in the ac-plane; however, the inclination with respect to the a-axis is now about 37°. In addition two incommensurate (IC) phases with a propagation vector $\boldsymbol{k} = (-0.214, 0.5, 0.457)$ were observed: AF2 between 8.0 K and 12.3 K and AF3 between 12.3 K and 13.5 K. The only difference between the IC-phases AF1 and AF2 arises from the orientation of the moments. These results were discussed in the frame of the ANNNI (axial next-nearest-neighbour Ising) model, which describes similar features as observed in $MnWO_4$: a large stability of a fourfold periodicity along a crystallographic axis and transitions to phases with different propagation vectors with increasing temperature and magnetic field strength. It will be noted that the ANNNI model is based on a uniaxial system and the Mn ion has probably only a weak anisotropy.

In the mixed system $Mn_{1-x}Fe_xWO_4$ two antiferromagnetic phases were observed simultaneously over the miscibility range $0.12 < x < 0.32$ [2, 3]. The magnetic Bragg intensities measured by neutron diffraction were related to the low temperature magnetic structure of $MnWO_4$ and to the magnetic structure of $FeWO_4$.

The occurrence of different magnetic phases in $MnWO_4$ and the coexistence of different magnetic structures in the mixed system $Mn_{1-x}Fe_xWO_4$ with low iron concentration motivated us to look in more detail at the magnetic behaviour. Here, we report on measurements of the magnetization, the specific heat and in particular on neutron diffraction studies at a $Mn_{0.88}Fe_{0.12}WO_4$ single crystal. Additionally, neutron powder diffraction studies on specimens with a similar composition are also reported.

2. Preparation and sample characterization

A single crystal of $Mn_{0.88}Fe_{0.12}WO_4$ with overall dimensions $4 \times 5 \times 15$ mm^3 was used for our measurements. The sample was characterized by electron probe microanalysis (EPM) and single-crystal neutron diffraction. The EPM measurements were performed at six different positions on the crystal surface. The result of the analysis at the different positions agrees within the experimental precision of 3% with respect to the concentration of the elements. The average concentration of Fe and Mn was determined to be 0.12 ± 0.01 and 0.86 ± 0.01, respectively.

A small part with overall dimensions $3 \times 4 \times 5$ mm^3, henceforth referred to as the small single crystal, was cut from the large crystal and was used for neutron four-circle diffraction on the instrument E5 at BENSC using $\lambda_n = 0.912$ Å. Lattice constants were $a = 4.814(3)$ Å,

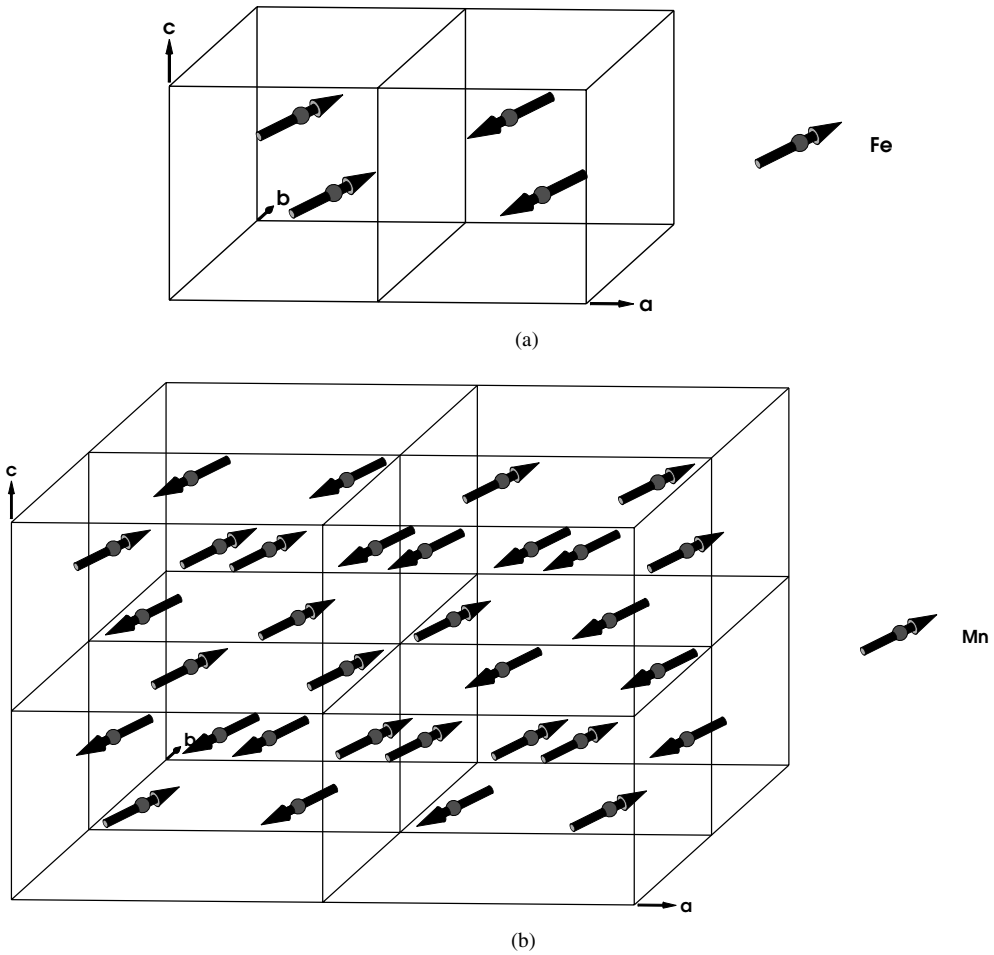

Figure 2. Magnetic structure of $FeWO_4$ (a) and $MnWO_4$ (b). Frames indicate the crystallographic unit cells in (a) and the unit cell doubled along a in (b).

$b = 5.7363(3)$ Å, $c = 4.982$ Å and $\beta = 90.95(6)^\circ$. A data set of 515 reflections (376 unique reflections) was collected at room temperature and subsequently refined in the space group $P2/c$ using the program Xtal 3.4 [4]. During the last refinement cycles a total of 33 parameters was refined: the scale factor, eight positional and 20 anisotropic thermal parameters, the g-value of extinction and the occupancy of the Fe/Mn and the two O sites, respectively. The crystal structure could be successfully refined resulting in residuals of $R_F = 0.032$ and $R_w = 0.020$ (table 1). Expecting a full occupancy of the 2f position by Fe and Mn atoms the ratio $x(\text{Fe})/(1-x)(\text{Mn}) = 0.123/0.877$ could be determined in agreement with the EPM results. Another indication for the sample homogeneity was obtained from the sharp magnetic phase transition at $T_N = 15.5$ K and a preliminary analysis of the critical behaviour corroborated the good homogeneity of our sample with a statistical distribution of the Mn and Fe atoms. Using a Gaussian distribution with a width Δx for the concentration x in $Mn_{1-x}Fe_xWO_4$ we could estimate a value of Δx below 3×10^{-3} [5].

Besides the measurements on the single crystal, powder samples of similar content were studied by neutron diffraction as well. These specimens were prepared by solid state reaction:

Table 1. Crystal structure parameters of $Mn_{0.88}Fe_{0.12}WO_4$. The anisotropic temperature factors are of the form $\tau_i = \exp[-2\pi^2(U_{11}h^2a^{*2} + \cdots + 2U_{13}hla^*c^*)]$ with U_{ij} quoted in [100 Å^2]. The numbers given in parentheses are the standard deviations obtained from the least squares analyses.

Atom	$P2/c$	x	y	z	Occup.	U_{11}	U_{22}	U_{33}	U_{12}	U_{13}	U_{23}
Mn	2f	1/2	0.6891(4)	1/4	0.877(2)	0.55(10)	0.52(10)	0.47(16)	—	−0.29(11)	—
Fe	2f	:	:	:	0.123(2)	:	:	:	—	:	—
W	2e	0	0.180 11(15)	1/4	1	0.57(4)	0.38(4)	0.43(6)	—	−0.18(4)	—
O1	4g	0.210 92(12)	0.1025(1)	0.9419(2)	0.999(7)	0.73(2)	0.68(3)	0.60(3)	−0.16(2)	−0.38(3)	0.12(2)
O2	4g	0.251 15(12)	0.3745(1)	0.3933(2)	0.979(7)	0.70(2)	0.71(2)	0.58(4)	−0.18(2)	−0.07(3)	0.05(2)

appropriate portions of $MnWO_4$ and $FeWO_4$ were mixed and preheated at 1000 °C in inert gas for one hour. Then the preheated sample was ground and preheated two times at 1000 °C for six hours. The powdered product was sintered at 1000 °C for one week and finally quenched to room temperature. The quality of the specimens were tested by neutron powder diffraction at room temperature at the multicounter diffractometer E6 using $\lambda_n = 2.4$ Å and were determined to be of single phase. The composition was found to be $Mn_{0.87}Fe_{0.13}WO_4$ for the two prepared specimens. Lattice parameters for all specimens are listed in table 2.

Table 2. Lattice parameters of $Mn_{1-x}Fe_xWO_4$ powders.

	$MnWO_4$	$FeWO_4$	$Mn_{0.87}Fe_{0.13}WO_4$
T [K]	1.6	80	20
a [Å]	4.834(1)	4.739(1)	4.825(1)
b [Å]	5.767(1)	5.716(1)	5.756(1)
c [Å]	5.005(1)	4.962(1)	5.010(1)
β [°]	91.13(7)	89.80(2)	90.88(8)

3. Specific heat and magnetization measurements

The specific heat was measured with a commercial MagLab heat-capacity system (Oxford Instruments) where the heat capacity is calculated from a thermal transient measurement. Measurements were performed on a small platelike single crystal at zero field in the temperature range from 1 K to 100 K. We observed an edge in the temperature dependent specific heat at 15.5 K and a cusp around 13.8 K (figure 3). In order to obtain some information on the phase diagram in the (H, T)-space magnetic fields up to 9 T were applied in the ac-plane. All measurements indicate two transition points, which both shift to lower temperature and approach each other with increasing field. At 9 T the transition points are at about 12.0 K and 11.3 K.

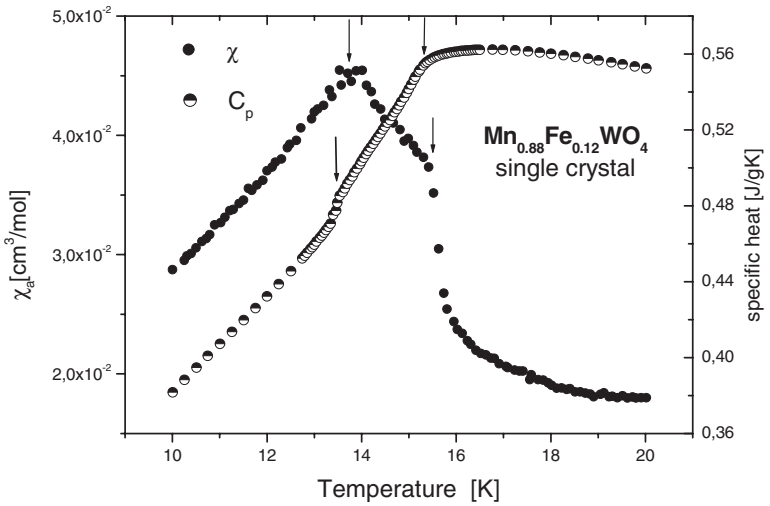

Figure 3. Susceptibility and specific heat of $Mn_{0.88}Fe_{0.12}WO_4$. Arrows indicate the presence of magnetic phase transitions. Differences in temperature between the specific heat and the magnetization data may be related to temperature sensor calibrations.

Table 3. Magnetic structure parameters for $Mn_{1-x}Fe_xWO_4$ powders. The quantities M, φ, $\boldsymbol{k}$ and R_M denote the mean magnitude of the moment, its angle in the ac-plane with respect to the a-axis, the propagation vector $\boldsymbol{k}$ and the residual for the squared structure factor.

	$Mn_{0.87}Fe_{0.13}WO_4$	$MnWO_4$	$FeWO_4$	$Mn_{0.87}Fe_{0.13}WO_4$
T [K]	1.5	1.5	1.5	14
M [μ_B]	4.5(1)	4.4(1)	4.7(1)	2.9(1)[a]
φ [°]	28(1)	37(1)	26(1)	17(2)
k	(1/4, 1/2, 1/2)	(1/4, 1/2, 1/2)	(1/2, 0, 0)	(0.232, 0.5, 0.508)
R_M [%]	8.8	7.8	6.1	6.2

[a] Fourier amplitude for the sinusoidally modulated structure.

Measurements of the magnetization were carried out using a commercial SQUID magnetometer (Quantum Design Company). A powder sample as well as a small single crystal with the field applied along the crystallographic a-, b-, and c-axis, respectively were studied. The dc-susceptibility was derived using $\chi = M/H$ and we checked for the linear behaviour of $M = \chi H$ for fields up to 2 T. A cusp in $\chi(H)$ is observed around 15.5 K and a second anomaly around 13.5 K in all our measurements (figure 3). The temperature dependent magnetization indicates the onset of an antiferromagnetic ordering below 15.5 K and a second magnetic phase transition around 13.5 K consistent with the behaviour found in the specific heat. The magnetization measurements were carried out under zero field cooling (ZFC) and field cooling (FC) conditions. A small hysteresis was found between ZFC and FC with a larger magnetization in the FC measurement. The effective paramagnetic moment for a $Mn_{0.88}Fe_{0.12}WO_4$ powder was determined to be about 6.0 μ_B by fitting the magnetization data between 50 K and 270 K to a Curie–Weiss law.

4. Neutron diffraction

Powder diffraction data were used to refine the magnetic structures of $Mn_{0.87}Fe_{0.13}WO_4$ at 1.5 K and 14 K. All measurements were performed on the E6-multicounter diffractometer using a double focusing pyrolytic graphite (PG) monochromator at wavelength $\lambda_n = 2.4$ Å. A PG filter was put in the beam to suppress second order contamination. The diffraction pattern was collected in the 2θ range between 10° and 90°. Rietveld analyses of the magnetic and nuclear structures were then carried out with the Fullprof program [6]. The magnetic reflections observed in the powder pattern at 1.5 K could be indexed with respect to a magnetic unit cell of dimensions $4a \times 2b \times 2c$ similar to the low temperature magnetic phase of pure $MnWO_4$ [1]. Using the collinear sinusoidally modulated magnetic structure of $MnWO_4$ with the moments confined to the ac-plane as input to our analysis we obtained a satisfactory fit to the data (table 3). The magnetic structures determined from powder measurements of the pure $MnWO_4$ and $FeWO_4$ compounds are also listed in table 3.

The temperature behaviour of the diffraction pattern in the 2θ range from 10° to 30° was measured between 1.5 K and 16 K. A phase transition of the magnetic structure was found between 13 K and 14 K and Bragg reflections of magnetic origin were observed only up to 15.5 K. The propagation vector shifts above the transition. No indication was found for a third magnetic phase as observed in $MnWO_4$ [1]. A pronounced temperature hysteresis occurs between 13 K and 14 K across the phase transition. The high temperature magnetic phase in $Mn_{0.87}Fe_{0.13}WO_4$ was determined at 14 K (figure 4 and table 3). Again the moments were constrained in our analysis to be in the ac-plane; however, different from the data collected at 1.5 K the two components $\boldsymbol{k}_x$ and $\boldsymbol{k}_z$ of the propagation vector $\boldsymbol{k}$ were used

as free parameters during the Rietveld refinement while the component $\boldsymbol{k}_y$ was fixed to 0.5 considering the monoclinic symmetry. We obtained a good fit to the data and the propagation vector of the incommensurate structure was refined to $\boldsymbol{k} = (0.232, 1/2, 0.508)$.

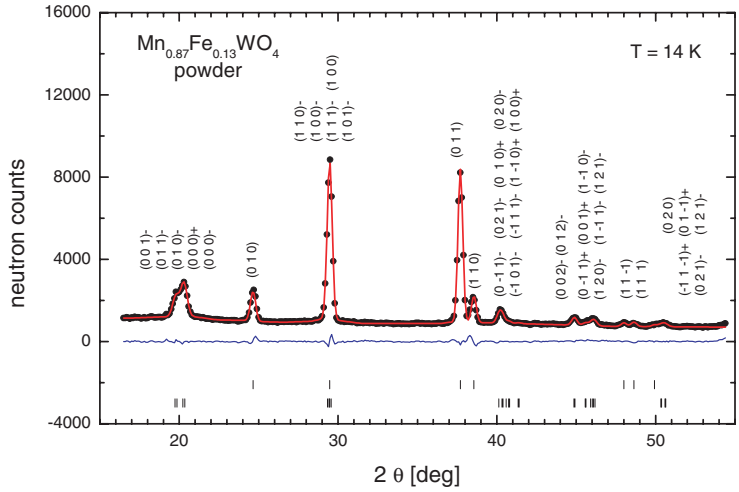

Figure 4. Neutron powder diffractogram with fit and difference pattern of $Mn_{0.88}Fe_{0.12}WO_4$. Upper and lower row of bars in the lower part of the figure mark positions of nuclear and magnetic reflections, respectively. The +/− at the reflection indices indicate magnetic satellites as $(h\,k\,l)^{\pm} = (h\,k\,l)_N \pm \boldsymbol{k}$.

Four-circle diffractometry at the instrument E5 was applied to study the magnetic phases at the small single crystal of $Mn_{0.88}Fe_{0.12}WO_4$. The specimen was mounted in a closed-cycle refrigerator. One data set consisting of 55 magnetic reflections was collected at 11 K using the propagation vector (0.25, 0.5, 0.5) for the low temperature magnetic structure as observed in the neutron powder diffraction. A second data set consisting of 45 magnetic Bragg reflections was measured at 14 K to analyse the high temperature magnetic phase. Three parameters, the Fourier amplitude M for the magnetization, the moment direction within the ac-plane defined by the angle φ and the fractional coordinate y of the (Mn,Fe) position were determined from a least squares fit of the integrated intensities using the magnetic structure models obtained in the neutron powder diffraction (table 3). The results of the single-crystal data analyses are in good agreement with those obtained from the Rietveld analyses of the powder data sets.

The temperature variation of the magnetic propagation vector around the transition at 13.5 K was studied in detail on the diffractometer E6. Magnetic Bragg diffraction around the reciprocal lattice point (r.l.p.) $(1/4\,1/2\,1/2)$ was measured by ω-scans. The peak position across the C–IC phase transition is shown in figure 5 for a measurement with increasing temperature. In the measurement with decreasing temperature the transition looks similar; however, it is shifted by about 0.5 K to lower temperatures. Characteristic for the transition is the sharp kink close to 13.6 K. The shift of the propagation vector with approach to the IC–C transition temperature indicates a logarithmic behaviour and can be described by $K = c_1 \ln(T - T_0) + c_2$ as indicated in figure 5. The peak shape of the ω-integrated intensity can be described by a pseudo-Voigt function. The FWHM changes from 0.26° below 13.5 K to 0.29° between 13.6 K and 14.5 K.

The observation of a possible coexistence of a ferberite-type and a huebnerite-type antiferromagnetic structure in $Mn_{1-x}Fe_xWO_4$ stimulated us to look for $(h/2\,k\,l)$ reflections too [2]. These measurements were performed on the instrument E7 of BENSC and the

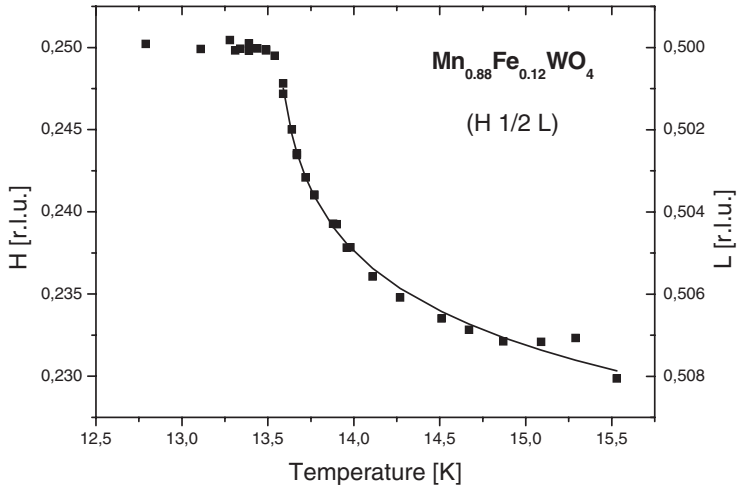

Figure 5. Temperature behaviour of the magnetic propagation vector of $Mn_{0.88}Fe_{0.12}WO_4$ across the IC–C phase transition for the dominating $MnWO_4$-type phases measured with increasing temperature. The full curve indicates the fit using $K = c_1 \ln(T - T_0) + c_2$.

diffractometer D10 of the ILL. The triple axis spectrometer E7 was operated in a two-axis mode with removed analyser using an incoming wavelength $\lambda_n = 2.38$ Å. A PG filter 60 mm thick was put in front of the monochromator. In some scans a second PG filter of 40 mm was mounted in front of the detector to insure that second-order contaminations can be neglected. During the measurements the large single crystal was mounted in an Orange-type cryostat and oriented with the (1 0 0) and (0 1 1) nuclear reflection in the scattering plane.

Below 19 K Bragg reflections of type $(h/2\,k\,k)$ could be observed. We have measured the temperature dependence of the maximum intensity for the Bragg reflections (1/2 0 0), (1/2 1 1), (3/2 0 0) and (3/2 1 1) in the range between 1.5 K and 20 K (figure 6). These measurements indicate a gradual increase (no sharp phase transition!) of the reflections starting at 19 K and reaching a maximum around 15.5 K. Then the intensities decrease and nearly vanish around 13 K. Below 13 K the (1/2 0 0) reflection increases again up to a value at 1.5 K, which is approximately the intensity observed at 15.5 K. The relative increase in intensity towards lower temperature is less pronounced for the reflections (3/2 1 1) and (1/2 1 1) and absent for (3/2 0 0).

Data sets of reflections related to a structure with a propagation vector $(1/2, 0, 0)$ were then collected at about 16 K, 14 K and 2 K using the four-circle diffractometer D10 at the ILL. The measurements were performed with the large crystal mounted in the helium flow cryostat. A least squares fit with a data set of 292 nuclear reflections (71 unique reflections) measured at 2 K confirmed the crystal structure obtained from the analysis of the measurements at the small crystal at the E5 as described above and was needed to calibrate the size of the magnetic moment obtained from the analysis of magnetic Bragg diffraction. Data analysis was performed using the Cambridge Crystallographic Subroutine Library. All data sets, related to a structure with a propagation vector $(1/2, 0, 0)$ and measured at different temperatures, contained 94 reflections (31 unique reflections). We obtained a good fit to the data set at 16.5 K using an $FeWO_4$-type magnetic structure with the moment again confined to the ac-plane (table 4). A similar result was found at 14 K and is also quoted in table 4. For both temperatures the moment orientation agrees with the one determined for the $MnWO_4$-type structures in $Mn_{0.88}Fe_{0.12}WO_4$ as described above. It should be noted that at 16 K no $MnWO_4$-type structure is present while at

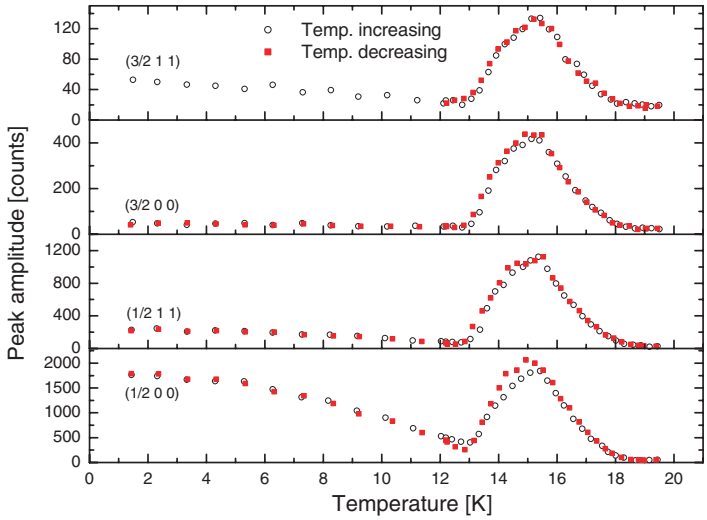

Figure 6. Temperature behaviour of the maximum peak intensity of magnetic Bragg reflections of type $(h/2\,k\,k)$.

14 K most spins are ordered in an IC $MnWO_4$-type structure. The size of the average moment in the $FeWO_4$-type structure amounts to 0.33 μ_B and 0.45 μ_B at 16 K and 14 K, respectively. The average moment at 15.5 K, the temperature of the onset of the dominating $MnWO_4$-type structure, was determined to be 0.6 μ_B. As can already be seen from the temperature behaviour of a few $(h/2\,k\,k)$ reflections the structure with $\boldsymbol{k} = (1/2, 0, 0)$ below 13 K differs significantly from the magnetic $FeWO_4$-type structure present above 13 K. Although the structure has not been solved yet we will mention a few remarkable points. First, the data set collected at D10 at 2 K shows that no (3/2 0 0) reflection is observed although the (1/2 0 0) and the (5/2 0 0) reflections are present. Since the (Mn^{2+},Fe^{2+}) ions occupy the 2f position in the space group $P2/c$ the x-coordinate is always 1/2, and magnetic Bragg reflections $(n+1/2\,0\,0)$ with n integer probing a magnetic order with a non-zero magnetic moment on the planes perpendicular to $x = 1/2$ should only differ in their inherent magnetic form factor. Therefore, a magnetic structure with moments localized at the crystallographic 2f position only cannot account for our observations. Second, reflections at positions like $(-1/2\,0\,1)$ occur, which in the case of a collinear magnetic structure would be present if e.g. the two moments in the chemical unit cell were antiparallel. For the $FeWO_4$-type structure the moments are parallel.

Table 4. Magnetic structure parameters for a $Mn_{0.88}Fe_{0.12}WO_4$ single crystal. The quantities M, φ, $\boldsymbol{k}$ and R_{magn} are defined in the caption of table 3. Numbers in parentheses of the second row give the used wavelength λ_n (Å).

	$Mn_{0.88}Fe_{0.12}WO_4$	$Mn_{0.88}Fe_{0.12}WO_4$	$Mn_{0.88}Fe_{0.12}WO_4$	$Mn_{0.88}Fe_{0.12}WO_4$
Diffractometer	D10(2.362)	D10(2.362)	E5(2.4)	E5(2.4)
T [K]	∼16	∼14	14	11
M [μ_B]	0.33(2)	0.45(2)	3.29(3)	4.14(2)
φ [°]	26(4)	23(3)	24.0(1)	23.7(7)
$\boldsymbol{k}$	(1/2, 0, 0)	(1/2, 0, 0)	(0.232, 0.5, 0.508)[a]	(1/4, 1/2, 1/2)
R_{magn} [%]	19	20	11.6	5.0

[a] Propagation vector taken from powder measurements of $Mn_{0.87}Fe_{0.13}WO_4$ for the '$MnWO_4$-type' structures, see table 3.

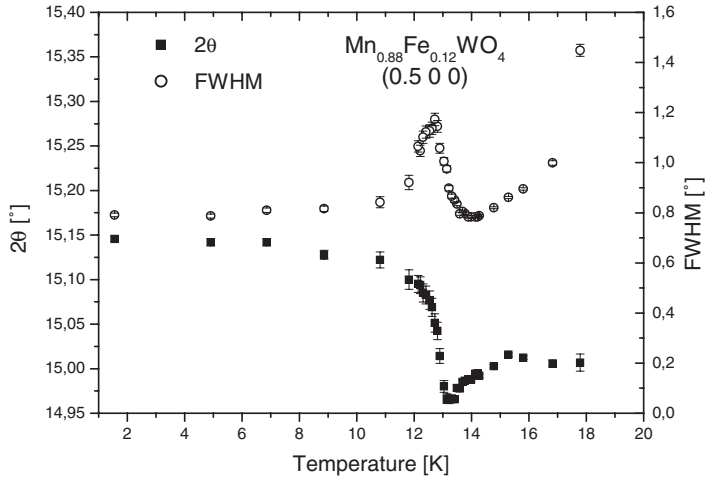

Figure 7. Temperature behaviour of the diffraction angle and the peak width (FWHM) of the magnetic '$(1/2, 0, 0)$' reflection.

Next we have followed the peak position and peak shape of the $(1/2\,0\,0)$ reflection in the whole temperature range between 18 K and 1.5 K. These measurements were performed with decreasing temperature on the instrument E6 and the diffraction was again measured in the reciprocal lattice plane $(h\,k\,k)$. All reflections were recorded by ω-scans. The ω-integrated peak profile as a function of the diffraction angle 2θ was then analysed in respect of its position and FWHM (figure 7). These analyses indicate that the position of the $(1/2\,0\,0)$ reflection decreases gradually in 2θ between 18 K and 13 K. Below 13 K the peak position changes sharply by more than 0.1° within a temperature interval of 0.5 K. Due to the small shift in the peak position it was not possible to determine the absolute value of $\boldsymbol{q}$ in the reciprocal lattice. Moreover our measurements were confined to the $(h\,k\,k)$ plane and we measured only projections onto this plane. The peak shape of the $(1/2\,0\,0)$ reflection above 16.5 K can be well described by a Lorentzian while the peak shape is predominantly Gaussian between 16.5 K and 13.2 K. Between 13.2 K and 12 K the intensity is small (figure 5) and the peak width broadens up to a FWHM of 1.2° at $T \approx 12.5$ K. Below 12 K we measure a mainly resolution limited Bragg intensity with a Gaussian lineshape.

5. Discussion

As already stated in the introduction the magnetic structure in $MnWO_4$ and $FeWO_4$ are quite different although they are chemically isostructural. A phenomenological description of relevant exchange paths to describe the observed collinear AF ground state of $MnWO_4$ with $\boldsymbol{k} = (\pm 1/4, 1/2, 1/2)$ was suggested in [7]: considering Goodenough–Kanamorii rules [8, 9] for the superexchange the coupling by the 90° exchange of Mn–O–Mn within the zig-zag chains along the c-axis should be undetermined and the structure is stabilized by couplings along various superexchange paths via two oxygen ions. Recently magnon dispersions obtained from inelastic neutron scattering were used to derive nine couplings via one or two oxygens [10]. These results support the view that the structure is stabilized by superexchanges via two oxygens between various Mn ions located in different zig-zag chains.

The collinear AF magnetic ground state of $FeWO_4$ with $\boldsymbol{k} = (1/2, 0, 0)$ was also explained phenomenologically by superexchange via one or two oxygen ions and the difference between the spin ordering in $MnWO_4$ and $FeWO_4$ was attributed to the different couplings of the Fe as compared to Mn ions [7]. E.g. the 90° superexchange along the zig-zag chains is expected to be strongly ferromagnetic for Fe while it is undetermined for Mn.

Former studies on the mixed system $Mn_{1-x}Fe_xWO_4$ indicated a coexistence of the $MnWO_4$- and $FeWO_4$-type magnetic structures in the concentration range $0.12 \leqslant x \leqslant 0.32$ [2]. In the latter work careful investigations of lattice constants and line widths by x-ray investigations of nuclear reflections showed the perfect miscibility of this system. In the mixed system one has to consider superexchange by Mn–Mn, Fe–Fe and Mn–Fe. According to Goodenough a 180° superexchange could be strongly antiferromagnetic for Mn^{2+}–Fe^{2+}, which would be similar to the coupling between Mn^{2+}–Mn^{2+} or Fe^{2+}–Fe^{2+} [8]. Therefore an intrinsic coupling of coexisting magnetic structures can be possible.

We will now turn to discuss our experimental observations of the complex magnetic behaviour in $Mn_{0.88}Fe_{0.12}WO_4$. The magnetization measurements and the specific heat (figure 3) indicate two phase transitions. Our neutron diffraction experiments show that the associated magnetic structures are closely related to the ones found in pure $MnWO_4$ [1]. The low temperature commensurate structure for $T \leqslant 13$ K corresponds to the magnetic ground state AF1 of pure $MnWO_4$ with $\boldsymbol{k} = (1/4, 1/2, 1/2)$, the only difference being the orientation of the moments in the ac-plane. In $Mn_{0.88}Fe_{0.12}WO_4$ the orientation of the moments with an inclination of about 26° to the a-axis is very close to the orientation in pure $FeWO_4$. This shows that the uniaxial anisotropy is determined by the Fe^{2+} ions and not by the Mn^{2+} ions. This is not surprising since the latter have a half filled d shell with vanishing orbital momentum. In $MnWO_4$ two incommensurate magnetic phases, AF2 between 8 K and 12.3 K and AF3 between 12.3 K and 13.5 K, were reported with the same propagation vector $\boldsymbol{k} = (-0.214, 1/2, 0.457)$. While the moments order in the ac-plane for AF3, a component along the b-axis exists for AF2 [1]. The absence of an AF2-like phase in $Mn_{0.88}Fe_{0.12}WO_4$ is probably related to the influence of the Fe^{2+} anisotropy, which may suppress a magnetization component along the b-axis. The presence of the Fe^{2+} ions also influences the propagation vector, which in our case is $\boldsymbol{k} = (0.232, 1/2, 0.508)$. Taking into account the mirror symmetry perpendicular to b for space group $P2/c$ this wave vector is equivalent to $\boldsymbol{k} = (-0.232, 1/2, 0.492)$ and can now be compared to $\boldsymbol{k} = (-0.214, 1/2, 0.457)$ for pure $MnWO_4$. The presence of the Fe^{2+} ions mainly decreases the shift Δl between the C and IC phase roughly by a factor of 5 while the reduction Δk amounts approximately to a factor of 2. In addition the transition temperatures rise from 8 K to 13 K for the IC–C transition and from 13.5 K to 15.5 K for T_N. The possible couplings to about 18 neighbours by nine geometrically different superexchange paths between statistically distributed pairs of Mn–Mn, Fe–Fe and Mn–Fe rule out a quantitative analysis although the crystal structure seems to be simple in the sense that the magnetic ions occupy only one symmetry equivalent position. The increase in all transition temperatures with the replacement of about 12% Mn by Fe shows that some Mn–Fe, or Fe–Fe couplings stabilize the magnetic $MnWO_4$-type structures. Within our experimental resolution we observed a continuous shift of the magnetic propagation vector as a function of temperature across the IC–C phase transition. Since it was speculated that $MnWO_4$ could be an ANNNI model system one has to consider this for $Mn_{0.88}Fe_{0.12}WO_4$ too. Both systems possess a commensurate $(+\ +\ -\ -)$ sequence of moments along the a-axis. Such a type of magnetic ordering is one of the ground states of the ANNNI model, which is a popular theoretical model investigated intensively in recent decades in order to understand general features of IC–C phase transitions observed in real systems [11, 12]. Basic to this model is a uniaxial anisotropy which is more pronounced in the $(Mn,Fe)WO_4$ systems than in the pure $MnWO_4$, a ferromagnetic nearest-neighbour interaction

J_1 and an antiferromagnetic next-nearest-neighbour interaction J_2. At low temperatures there exists an antiferromagnetic $(+\ +\ -\ -)$ ground state for $J_1 < -2J_2$ and a ferromagnetic one for $J_1 > -2J_2$. With increasing temperature successive commensurate phases appear before the system enters the paramagnetic phase. Within a description of the ANNNI model the smaller shift of Δk during the IC–C transition and the reduction in $(T_N - T_{IC-C})/T_N$ for $Mn_{0.88}Fe_{0.12}WO_4$ compared to $MnFeWO_4$ indicates a relative increase in the ratio of $-J_2/J_1$ due to the addition of the Fe^{2+} ions. It was found from the peak shape analysis that the peak shape in the IC phase slightly deviates from the one in the C phase. Therefore an 'infinite' long range order seems not to be present in the IC phase.

Now we will consider the reflections observed at r.l.p. $(h/2\,k\,k)$ below 19 K pointing to an $FeWO_4$-type spin ordering. It was found earlier from studies on the magnetic behaviour of $Fe_{1-x}Mg_xWO_4$ that the substitution of Fe by the diamagnetic Mg destroyed long range order for a concentration of Fe below 25% [2]. Hence the content of about 12% Fe^{2+} ions is well below the percolation limit and the presence of the $FeWO_4$-type magnetic structure between 13 K and 19 K has to be promoted by superexchange interactions involving Mn^{2+} ions too. The gradual increase in the diffraction intensities from 19 K towards 15.5 K accompanied by a decreasing linewidth suggests an ordering of Fe^{2+} and Mn^{2+} ions on 'diluted' three-dimensional clusters probably extending in their linear extension with decreasing temperature. Therefore the magnetic behaviour is expected to have some features of a system of low dimensionality $(d < 3)$. With the onset of an ordered $MnWO_4$-type magnetic structure at 15.5 K the decrease in the $(h/2\,k\,k)$-type reflections and the broadening of the peak shape show that already ordered magnetic moments change their orientation to become incorporated into the $MnWO_4$-type magnetic structure and the linear extension of the magnetically ordered $FeWO_4$-type clusters shrinks. Due to the homogeneity of the specimen and the strongly correlated temperature behaviour of the two different structures between 15.5 K and 13 K most spins are ordered in one of the two possible structures. Therefore both structures are homogeneously superimposed and supposed to interpenetrate each other. The possibility of such a simultaneous ordering was discussed within mean field theory earlier [13]. At 13 K the $(h/2\,k\,k)$ reflections nearly vanish and the spins seem to be mainly ordered in the $MnWO_4$-type structure. Very surprising is the recurrence now of $(h/2\,k\,l)$ reflections below 13 K, which cannot originate from a 'pure' magnetic $FeWO_4$-type structure. In particular a Bragg peak is present at $(1/2\,0\,0)$ and $(5/2\,0\,0)$ while no peak was observed at $(3/2\,0\,0)$. As already mentioned in the foregoing section this observation is in contradiction with a magnetization distribution with moments purely localized on the (Mn,Fe) 2f positions. It may now be speculated whether this unusual behaviour can originate from a magnetization distribution carried by intinerant charge carriers.

6. Summary and concluding remarks

From our experimental investigations we can draw the following qualitative picture of the magnetic behaviour in $Mn_{0.88}Fe_{0.12}WO_4$. A 12% substitution of Fe on the Mn position leads to an interesting competition between and a coexistence of interpenetrating magnetic structures related to the pure systems $MnWO_4$ and $FeWO_4$. This behaviour results from superexchange couplings between Mn–Mn, Fe–Fe and Mn–Fe via one or two intervening oxygen ions. Dependent on the path, the Mn–Mn, Fe–Fe or Mn–Fe coupling by superexchange can be of the same sign (i.e. ferro or af) in some cases and of opposite sign in other cases. Therefore a cluster-like $FeWO_4$-type ordering becomes possible although the Fe concentration is well below the percolation limit. The $FeWO_4$-type ordering interpenetrates the $MnWO_4$-like magnetic structure dominating the spin ordering below 15.5 K. The intimate coupling of both structures is proved by the strong correlation in the temperature behaviour of the corresponding

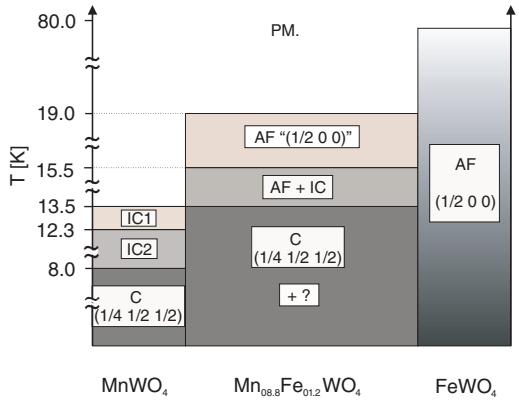

Figure 8. Magnetic phases of $MnWO_4$ [1], $Mn_{0.88}Fe_{0.12}WO_4$ and $FeWO_4$. The magnetic propagation vector for IC1 and IC2 is $\boldsymbol{k} = (-0.214, 0.5, 0.457)$, and $\boldsymbol{k} = (0.232, 0.5, 0.509)$ for IC.

Bragg intensities. Essential for such a behaviour is the much stronger Fe–Fe coupling in comparison to Mn–Mn, combined with a small Fe/Mn occupancy on the 2f transition metal position.

The IC–C phase transition as observed in pure $MnWO_4$, which was discussed within the frame of the ANNNI model [1], is significantly influenced by the substitution of Fe. A comparison of this transition for $MnWO_4$ and $Mn_{0.88}Fe_{0.12}WO_4$ was not possible due to a lack of a suitable $MnWO_4$ single crystal. An earlier investigation on the magnetic phases in pure $MnWO_4$ by another group does not explicitly address the temperature behaviour of the propagation vector [1].

The observation of a $(1/2\,0\,0)$ and $(5/2\,0\,0)$ and the absence of the $(3/2\,0\,0)$ reflection at low temperatures is in strict contradiction to a magnetization distribution of local moments at the 2f positions of the (Mn,Fe) ions. This remarkable behaviour will be studied further in the future. A summarizing overview of the different magnetic phases in $Mn_{0.88}Fe_{0.12}WO_4$ including also the known phases of the end members $MnWO_4$ and $FeWO_4$ is shown in figure 8.

Acknowledgments

We thank Professor D Hohlwein, Professor K D Schotte and Dr U Schotte for critical reading of the manuscript and D Wilhelm for performing the electron probe microanalysis.

References

[1] Lautenschläger G, Weitzel H, Vogt T, Hock R, Böhm A, Bonnet M and Fuess H 1993 *Phys. Rev.* B **48** 6087 and references therein
[2] Obermayer H A, Dachs H and Schröcke H 1973 *Solid State Commun.* **12** 779
[3] Ding Y *et al* 2000 *Physica* B **276** 596
[4] Hall S R, King G S D and Stewart J M (ed) *XTAL* 3.4, University of Western Australia, Lamb, Perth
[5] Ding Y 1999 *Thesis* Technical University Berlin
[6] Rodriguez-Carvajal J, FullProf: a program for Rietveld refinement and pattern matching analysis *Abstract of the Satellite Meeting on Powder Diffraction on the 15th Congress of the IUCr (Toulouse, 1990)* p 127
[7] Weitzel H and Langhof H 1977 *J. Magn. Magn. Mater.* **4** 265
[8] Goodenough J B 1963 *Magnetism and Chemical Bond* (New York: Wiley)
[9] Kanamori J 1959 *J. Phys. Chem. Solids* **10** 87

[10] Ehrenberg H, Weitzel H, Fuess H and Hennion B 1999 *J. Phys.: Condens. Matter* **11** 2649
[11] Selke W 1992 *Phase Transitions and Critical Phenomena* vol 15, ed C Domb and J L Lebowitz (New York: Academic)
[12] Bak P 1982 *Rep. Prog. Phys.* **45** 587
[13] Wegner F 1973 *Solid State Commun.* **12** 785